

MICROSTRUCTURE CONTROL DURING SINGLE CRYSTAL LASER WELDING AND DEPOSITION OF NI-BASE SUPERALLOYS

S.Mokadem¹, C. Bezençon¹, J.-M. Drezet^{1,2}, A. Jacot^{1,2}, J.-D. Wagnière¹, W. Kurz¹

¹ Ecole Polytechnique Fédérale de Lausanne ; 1015 Lausanne EPFL, Switzerland

² Calcom ESI S.A. ; Parc Scientifique EPFL, 1015 Lausanne, Switzerland

Keywords: Superalloy, Laser treatment, single crystal growth

Abstract

In the Epitaxial Laser Metal Forming (E-LMF) process, metal powder is injected into a molten pool formed by controlled laser heating with the aim of producing a single crystal deposit on a single crystal substrate. It is a near net-shape process for rapid prototyping or repair engineering of single crystal high pressure/high temperature gas turbines blades. Single crystal repair using E-LMF requires controlled solidification conditions in order to prevent the nucleation and growth of crystals ahead of the columnar dendritic front, i.e., to ensure epitaxial growth and to avoid the columnar to equiaxed transition. In the follow-up of previous research of the authors new strategies for microstructure control during E-LMF will be presented; (i) for off-axis dendritic growth, (ii) for the case of growth competition of grains of different orientation and (iii) for cellular dendritic growth where secondary branches are missing. Control of these phenomena is of major importance for an effective industrial application of the E-LMF process. For this purpose, models have been developed and used in association with extended experimental observation to predict the expected solidification morphology for a given set of laser processing parameters. New microstructure features such as oriented-to-misoriented transition and the loss of epitaxy in the critical branching zone are presented and measures for avoiding the formation of spurious grains within the repaired zone are discussed.

Introduction

For maximum performance, high pressure/high temperature turbine blades are usually made of single-crystal (SX) Ni base superalloys. The use of these expensive components creates the need for a repair process allowing the re-establishment of the initial properties and the original microstructure of the damaged parts. It has been shown recently that single crystal deposition is possible by a laser metal forming (E-LMF) technique [1, 2]. In this process, superalloy powder is molten by a high intensity laser beam and solidifies on the treated surface (fig. 1a). With this technique a complex three-dimensional single crystalline clad of a given geometry with a sound and well-bonded interface can be deposited.

To guarantee a SX structure, a precise process control for insuring epitaxial columnar growth is essential. This has been achieved in previous work through experiment and analytical modeling relating the dendritic microstructure (columnar or equiaxed) to the solidification conditions (temperature gradient, G , and solidification velocity, V) [1-3]. This approach does not take into account (i) the local growth direction of the columnar front nor (ii) the growth competition between misoriented grains. Furthermore, the complex E-LMF process has been simplified to laser remelting or welding (fig. 1b) and thus only qualitative relationships between processing parameters (such as laser power, spot diameter, beam velocity, etc.) and solidification variables (G and V) have been given.

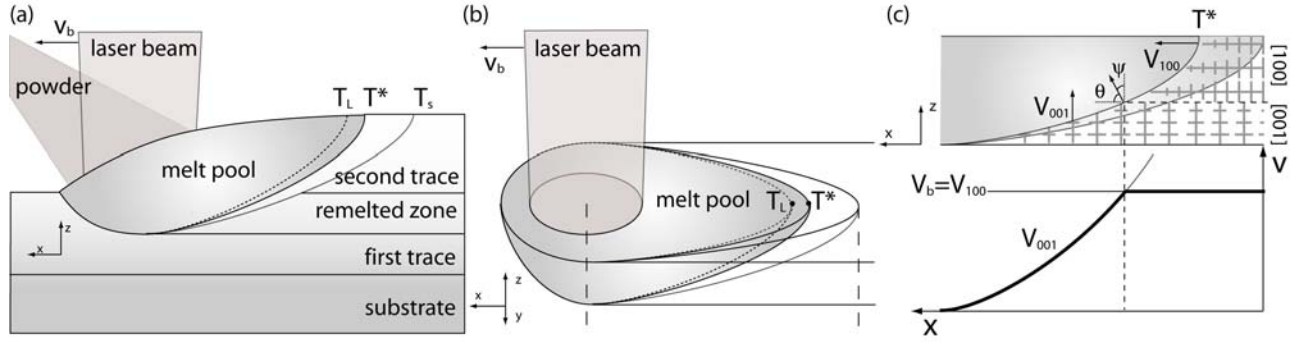


Figure 1. (a) Schematic representation of E-LMF process (first and second deposits are shown) and (b) laser remelting process. (c) Evolution of the solidification velocity within the melt pool for anisotropic dendrite growth. In all experiments, the laser beam motion defined by the vector v_b is parallel to $[100]$.

The objective of the paper is to present new results which are fundamental to a full process control of E-LMF. After a brief description of the laser metal forming and remelting process the major defects encountered during single crystal laser deposition, *i.e.*, loss of the crystal orientation of the substrate, is described taking into account the following aspects: off-axis dendritic growth, grain growth competition, and loss of epitaxy due to branching difficulties of cellular-dendritic structures.

Dendritic solidification of the melt pool

The solidification microstructure of the deposit is directly influenced by the solidification conditions prevailing at the transformation front, namely G and V . During laser treatment, the high energy density of the beam leads to high temperature gradients ($G \sim 10^5\text{-}10^7$ K/m) and laser beam velocities which are generally in the range of 1 to 100 mm/s. Under these conditions, the solidification morphology for nickel-base alloys is mainly dendritic or cellular-dendritic, either columnar or equiaxed (fig. 2) [4].

In cubic crystals, dendrites generally grow along one of the six $\langle 100 \rangle$ directions. The $\langle 100 \rangle$ orientation, which is closest to the heat flux direction, is selected as the dendrite tips grow then at the highest interface temperature (smallest undercooling). Therefore growth direction transitions may be observed, *i.e.*, secondary arms, which are orthogonal to the trunk, may become primary trunks as shown in fig. 1c and fig. 3b,c. In order to determine which of the $\langle 100 \rangle$ directions is selected at a given location of the melt pool, a geometrical relationship between the velocity of the dendrite tip, V_{hkl} , along a specific $[hkl]$ dendrite growth direction and the direction of the velocity vector of the laser beam V_b of the moving source is used [5] :

$$V_{hkl} = V_b(\cos\theta/\cos\psi) \quad (1)$$

where ψ is the angle between the isotherm normal and the dendrite growth direction and θ is the angle between the isotherm normal and the direction of the laser beam (see fig. 1c). The anisotropic growth behavior of the dendrite complicates the process control. Therefore in the following some new results and solutions to this problem will be discussed.

Microstructure control: new features

Experimental procedure

The influence of the crystal orientation on the microstructure development has been analyzed through laser remelting (which is close to welding and laser metal forming) of cylindrical SX samples machined from bars of commercial SX Ni-base superalloys of the first (CMSX-2) and second generation (MC2 and CMSX-4) which have been fully heat-treated (solutionized and aged). The cylinder axis (i.e. the casting direction) was approximately parallel to $\langle 100 \rangle$ with less than 10° deviation.

In this work, different substrate orientations defined as $\langle 100 \rangle(001)$ and $\langle 100 \rangle(011)$, where the index of the plane is parallel to the treated surface, have been investigated. A precise measurement of the substrate orientation with respect to the laser beam motion was done *a-posteriori* by electron backscattered diffraction (EBSD).

Laser treatment was undertaken with a 1.7 kW continuous CO₂ laser at scanning speeds $1 < V_b < 100$ mm/s. The laser beam had a near top-hat mode (TEM00 + TEM01) and a circular polarization. Experiments were performed on substrates at room temperature or with a preheating to $T_0 = 1000^\circ\text{C}$. The substrate temperature was controlled by induction heating. Treatments were carried out under a laminar flow of Ar for oxidation protection of the melt pool. Transverse sections of remelted traces were observed by optical microscopy, etched in a HCl-HNO₃-MoO₃ solution (Al-rich etching) and analyzed using EBSD.

Avoiding the CET in off-axis columnar dendritic growth

Careful selection of the processing parameters is required to insure (i) epitaxy between substrate and deposit through remelting of the substrate, and (ii) to avoid nucleation and growth of misoriented dendritic grains (CET). In this work, columnar and equiaxed dendrite growth was considered to follow the same relationship (thermal diffusion was neglected) and growth kinetics were obtained from the Ivantsov-Marginal Stability (IMS) - multicomponent model [6, 7] coupled with a thermodynamic database for Ni-base superalloys [8] using *ThermoCalc* [9]. Nucleation has been simplified by assuming that all heterogeneous nucleation sites are activated when the liquid undercooling is higher than a critical nucleation undercooling. The nucleation site density was determined by optical microscopy of laser remelting experiments and a randomly uniform nuclei distribution was assumed. Following Hunt [10], the maximum radius of the equiaxed grain is calculated by integration of the equiaxed velocity from the nucleation time, t_0 , to the time that the columnar front reaches the grain.

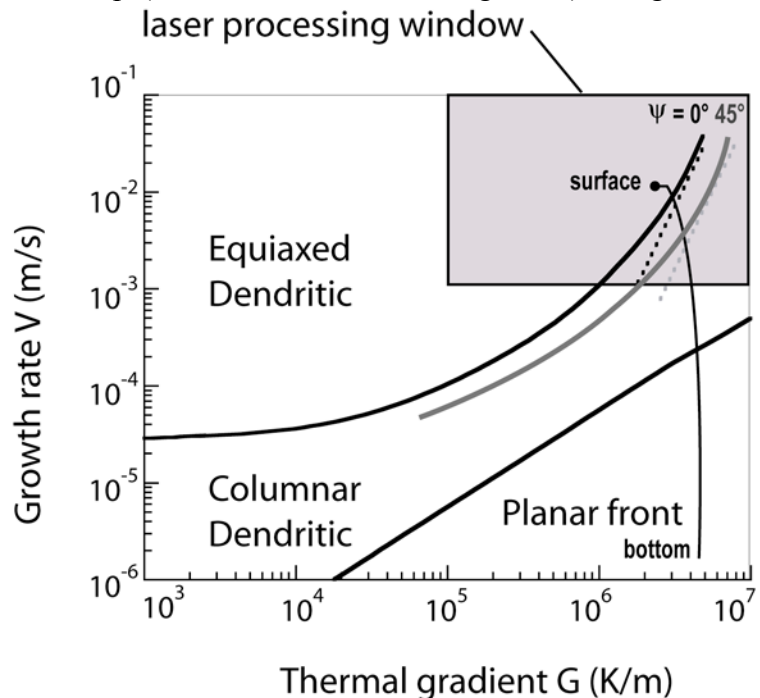


Figure 2. Microstructure selection map for the second generation superalloy CMSX4, showing the expected solidification morphology as a function of solidification conditions.

After substitution of time by the velocity dependent undercooling and integration the following criterion for a columnar regime is obtained :

$$G > \frac{2 \cdot N_0^{1/3} \Delta T_{col}^{n+1}}{(n+1) a \Delta T_0^n V_{iso}} \cdot \left(1 - \left[\frac{\Delta T_n}{\Delta T_{col}} \right]^{n+1} \right) \quad (2)$$

with G , the temperature gradient, ΔT_n , the nucleation undercooling, N_0 , the number of nucleation sites, a and n , alloy parameters and ΔT_{col} the dendrite tip undercooling. Fig. 2 shows the limit of columnar growth in the usual G - V -map and superimposed on it typical solidification conditions for the laser remelting process.

Taking into account anisotropic growth leads to columnar dendritic undercooling :

$$\Delta T_{col} = \Delta T_0 (a \cdot V_{hkl})^{1/n} = \Delta T_0 \left(\frac{a \cdot V_{iso}}{\cos \psi} \right)^{1/n} \quad (3)$$

Substituting this relationship into eq.2 one obtains a new criterion which is shown in figure 2. Off-heat flux growth due to crystal anisotropy ($\psi=45^\circ$) extends the equiaxed regime to higher G and lower V values.

Under solidification conditions encountered during laser treatment, ΔT_{col} is much larger than ΔT_n and the volume fraction, ϕ_{eq} , of equiaxed grains is mainly controlled by N_0 rather than ΔT_n [10, 11]. By neglecting ΔT_n it is found that ϕ_{eq} becomes a function of a ratio of the solidification conditions of the form of $G^n/V_{iso} (\cos \psi)^{n+1}$. The criterion for columnar growth under laser processing conditions (for high G and high V) can be expressed as follows [12], where the constant K_{CET} is a function of alloy parameters and of a transition criterion ϕ_c corresponding to the critical volume fraction of equiaxed grains :

$$\frac{G^n}{V_{iso}} (\cos \psi)^{n+1} > K_{CET} \quad \text{with} \quad K_{CET} = a \cdot \left[\left(\frac{-4\pi N_0}{3 \ln(1-\phi_c)} \right)^{1/3} \frac{\Delta T_0}{n+1} \right]^n \quad (4)$$

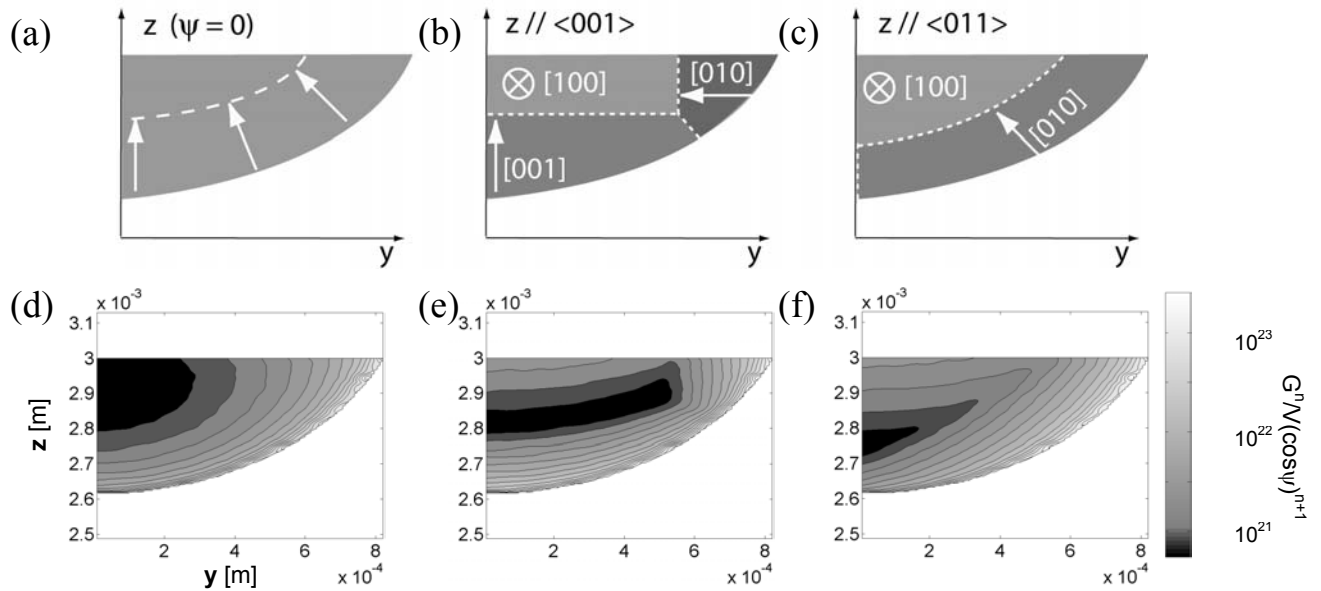


Figure 3. Spatial distribution of $G^n/V(\cos \psi)^{n+1}$ ratio (left side of eq.4) as a function of the position in the melt pool (transverse view) simulated through FEM for processing conditions : power 1700 W, scanning speed $v_b = 5$ mm/s, beam diameter $D_b = 2$ mm, substrate temperature $T_0 = 25^\circ\text{C}$, absorption $\beta = 13\%$. (a) Isotropic growth ($\psi=0$) (b) anisotropic growth, substrate orientation $\langle 100 \rangle (001)$ and (c) substrate orientation $\langle 100 \rangle (011)$.

When the heat-flux is not parallel to the dendritic growth direction given by the substrate, the dendrite tip velocity, V_{hkl} , is higher than the velocity normal to the solidification front by $(\cos\psi)^{-1}$. Thus, the critical K_{CET} as defined by the left hand side of eq.4 in the melt pool at liquidus temperature depends on the crystal orientation and is different from one defined by Hunt [10] and Gäumann [11] for isotropic growth ($\psi = 0$, fig. 3a). In fig. 3d, it is seen that the position of the minimum value of this CET ratio (black) is at the center and the rear of the melt pool when isotropic growth is assumed. It is close to the transition between two growth domains (c.f. fig. 3b, e and c, f) when anisotropic growth along defined crystal orientations is taken into account (see also fig. 2). It demonstrates that a cube growth direction transition is critical for nucleation and growth of spurious (equiaxed) grains, a result which is experimentally verified [12].

Grain competition

A new feature of the present research is that the loss of crystallographic orientation presented above cannot be correctly interpreted using the simplified CET model only. The growth competition during solidification between oriented columnar (epitactic) and misoriented columnar dendrites is of major importance *i.e.* in a strong temperature gradient the equiaxed grains become elongated, forming a polycrystalline columnar zone. In order to study this mechanism of growth competition a model developed by Rappaz and co-workers [13] that combines FE analysis with cellular automaton technique (CAFE) was used. In this way the influence of the misorientation of the $\langle 100 \rangle$ orientation of the SX with respect to the heat flux on the loss of epitaxy (here called oriented to misoriented transition, OMT) could be characterized.

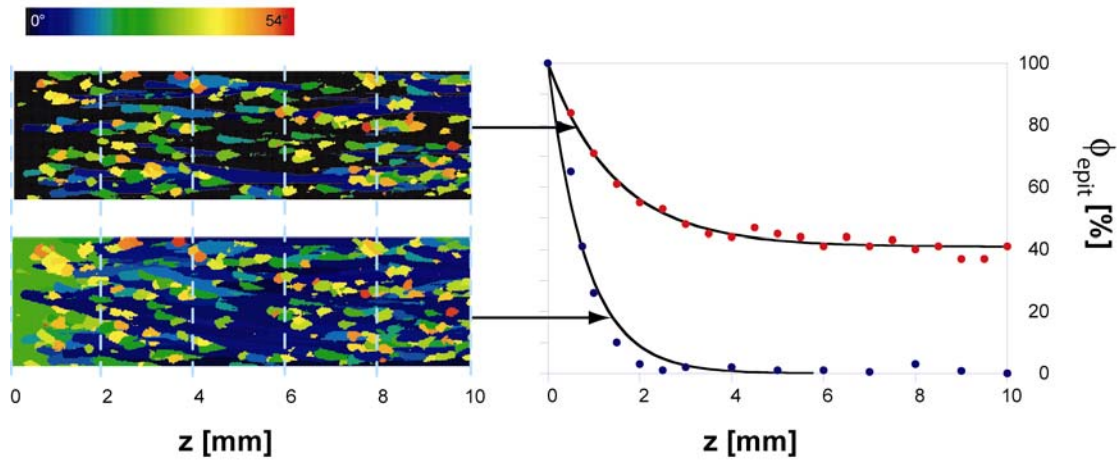


Figure 4. Calculated evolution of the epitactic fraction (volume fraction of grains whose crystallographic orientation equals that of the crystal seed) as a function of the length of a Bridgman sample for two different crystal seed orientations: $[100]$ parallel to the cylinder axis *i.e.* $\psi = 0^\circ$ (top) and $[110]$ crystallographic direction parallel to the solidification axis *i.e.* $\psi = 45^\circ$ (bottom), CMSX-4, $\Delta T_n = 9K$, $N_0 = 3.4e^{10} m^{-3}$, $G = 3e^4 K/m$, $V = 10 mm/s$.

It is shown that for a large angle between the heat flux direction and the dendrite growth direction, OMT may occur by growth competition leading to a new polycrystalline columnar structure and therefore to the loss of the initial crystallographic orientation of the substrate [14]. Figures 4 and 5 show this growth selection for a Bridgman type solidification with constant velocity and temperature gradient. The solidification in these calculations is initiated at the left (figure 4) with a given crystallographic orientation (single crystal seed) and finishes at the right. The growth competition selection occurs after the entrapment of equiaxed grains which

nucleate in the constitutionally undercooled zone ahead of the columnar front. These equiaxed grains develop antiparallel to the macroscopic heat flux and lead to a new columnar zone.

In the CET model, equiaxed grains once nucleated develop with various volume fractions depending on solidification conditions. They are incorporated into the columnar zone for small volume fractions or supersede it at high volume fraction. The OMT model, through the consideration of growth orientation and overgrowth, shows that during off-axis growth the epitactic fraction drops. The resulting microstructure is in this case defined by a competition between oriented (epitactic) and misoriented columnar grains. The position at which the transition between oriented and exclusively misoriented structure is taking place is strongly dependent on the crystallographic orientation of the substrate with regard to the heat flux (fig. 5).

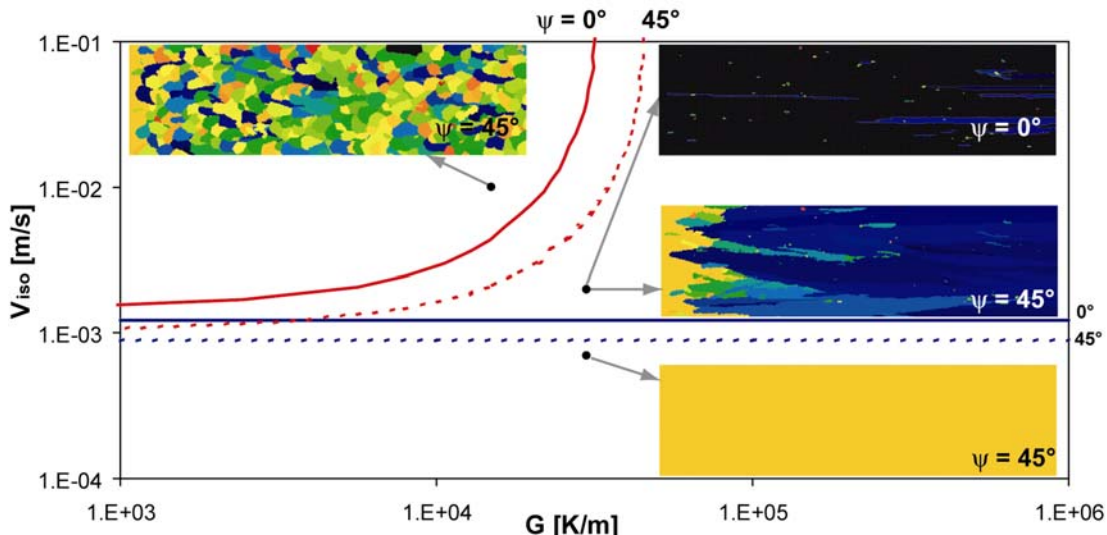


Figure 5. Microstructure map computed for CMSX-4 ($\Delta T_n = 9\text{K}$, $N_0 = 3.4e^{10} \text{ m}^{-3}$, $\phi_c = 0.49$) and results of CAFE modeling for three different solidification conditions (black points). Limits of the equiaxed domain as a function of the temperature gradient, G , the velocity of the liquidus isotherm, V_{iso} , and the angle between the dendritic crystallographic direction and the heat-flux, $\psi = 0^\circ$ and 45° , plain and dotted line respectively, are shown. The straight line (V_{iso} constant) depicts the lower limit under which the growth undercooling remains below the nucleation undercooling. The condition situated in the mixed regime shows an epitactic structure with some elongated spurious grains for well oriented sample whereas a sharp OMT takes place for $\psi = 45^\circ$.

Loss of epitaxy during off-axis growth related to branching

When the dendrite trunk axis is not aligned with the thermal flux during constrained growth (fig. 6b) the branching responsible for the formation of new primary trunks influences the local CET [15]. The dynamic competition between secondary and tertiary arms [16, 17] controls this phenomenon. Using a substrate with a [001] orientation not parallel to the heat flux (fig. 6b), a region of divergent growth forms (at the left in the figure). On this side the liquid can only solidify by the propagation of secondary branches and generation of new primary trunks from tertiary arms [17]. This phenomenon has been modeled for the control of stray grain formation in the platform of single crystal turbine blades [18].

The branching depends on composition, velocity, thermal gradient and orientation. If the growth conditions are such that branching is unlikely to occur, spurious grains nucleate (fig. 6c) and grow in the remaining liquid (fig. 7 C and D and corresponding EBSD maps). Control of this phenomenon is of major importance for an effective industrial application of the E-LMF process. For this purpose, the model of Bussac and Gandin [18] has been combined with the

columnar-to-equiaxed model [11]. This simple approach accounts for the fact that the dendrites growing along [001] away from the vertical wall form successive branches along the [010] direction covering a distance $\delta z(010)+\delta z(001)$ for an isotherm displacement δz (see fig. 6d) and thus experience a larger growth rate compared to dendrites growing along [001]. Two different expressions for the stationary grain envelope undercooling at the left and the right faces, respectively ΔT_{div} and ΔT_{conv} are then defined :

$$\Delta T_{div} = \Delta T_0 \left(a \cdot V_{iso} \cdot (\sin \psi + \cos \psi) \right)^{1/n} \quad \text{and} \quad \Delta T_{conv} = \Delta T_0 \left(\frac{a \cdot V_{iso}}{\cos \psi} \right)^{1/n} \quad (4a \text{ and } 4b)$$

This geometrical formulation of the problem allows an estimation of the expected solidification morphology for a given set of processing parameters. It allows also computation of microstructure diagrams as a function of the misorientation angle ψ and solidification velocity.

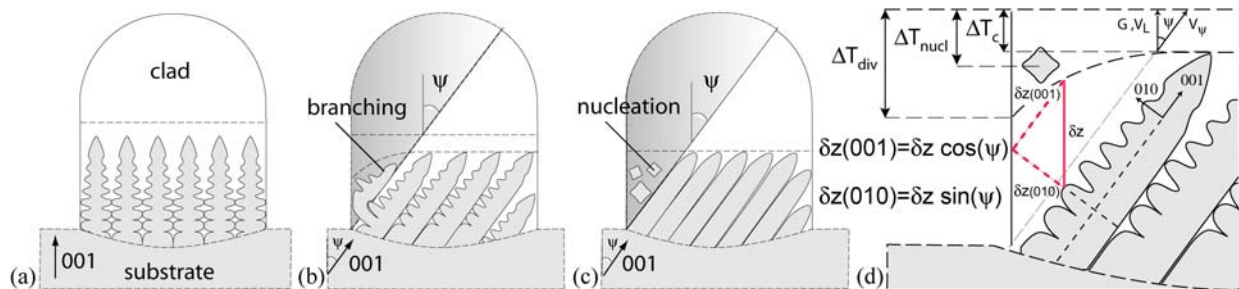


Figure 6. (a) Schematic representation of a transverse clad section for a well oriented substrate and (b) misoriented substrate experiencing off-axis growth with branching and (c) with nucleation in the critical branching zone. (d) Representation of convergent and divergent undercooling during off-axis growth : in order to reach a distance δz during a given time interval the dendritic network has first to follow [010] direction through a distance $\delta z(010)$ and next the distance $\delta z(001)$ in [001] direction.

The results of eq.2 and eq.4a-b, for an average constant temperature gradient ($3 \cdot 10^6$ K/m), are given in fig. 7. A lens-shaped region is obtained where loss of epitaxy in the critical branching zone may occur. At low velocity the microstructure is columnar and single crystalline, whereas at high velocity spurious grains are predicted.

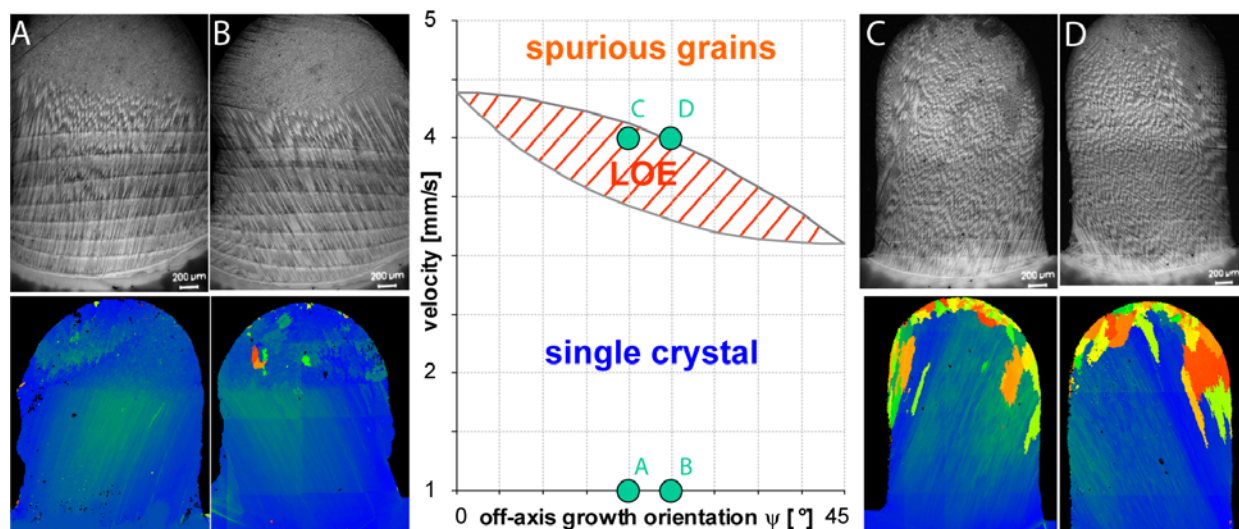


Figure 7. Microstructure map computed for CMSX-4 presenting the lens shaped region where loss of epitaxy in the critical branching zone may occur and experimental evidences of the phenomenon.

This simple model is in good agreement with experimental results obtained with CMSX-4 for different substrate orientations and laser beam velocities. The different average solidification conditions corresponding to these trials are lying in the columnar SX zone for samples A and B and in the loss of epitaxy (LOE) zone for sample C and D. However, experiments performed with superalloys MC2 and CMSX-2 (which are low ΔT_0 superalloys) show that LOE may occur even for conditions where only SX structure is predicted by the model. For these alloys and for the conditions encountered, the solidification morphology is cellular and the problem of side arm development through growth of morphological instabilities of the cells and of the secondary arms seems to be the limiting factor. Therefore a low ΔT_0 which is positive for [001] single crystal growth has a negative effect on off-axis growth.

Melt convection and dendrite fragmentation

The dendrite fragmentation process through remelting (thermal and/or constitutional) of secondary dendritic arms is expected to be also an important factor which strongly modifies the number of nucleation sites. Modeling of this phenomenon, which treats the constitutional remelting of secondary arms within the mushy zone, is ongoing for laser remelting.

Conclusions

In this work, a new criterion is proposed describing the extent of columnar growth as a function of the important solidification variables; G , V and the angle of the dendrite axis with respect to the isotherm norm, ψ . According to this criterion the highest risk for a loss of epitaxy is found to be close to growth direction transition zones where another $\langle 100 \rangle$ direction is selected. The risk of equiaxed grain formation (CET) is increased when ψ is increased.

The influence of orientation and growth competition on the fading of the epitaxial fraction during off-axis solidification has been analyzed through cellular automaton modeling of off-axis directional solidification. With this model the relation between the misorientation angle ψ and the position corresponding to the effective loss of epitaxial structure for given solidification conditions could be obtained. The results show that loss of crystallographic orientation within the melt pool cannot be correctly interpreted by the simple analytical CET model.

Moreover, the loss of epitaxy (LOE) in a specific area of the clad occurring when E-LMF is performed on off-axis oriented SX substrates has been shown. Taking into account the geometrical aspect of the phenomena, the use of convergent and divergent growth undercoolings led to a microstructure map showing a lens shaped domain in a $V(\psi)$ diagram within which LOE can occur. Although this latter result has been experimentally verified using superalloys with a large solidification interval, experiments realized on low solidification range superalloys show that the branching of cellular structures has to be taken into account in the latter case.

Acknowledgements

The authors thank A. Schnell, Alstom (Switzerland) Ltd, for his help in calculating the thermodynamic data for CMSX4.

References

- [1] Gäumann M. PhD Thesis. Institut of Materials: Swiss Federal Institut of Technology (EPFL); 1999.
- [2] Gäumann M, Bezençon C, Canalis P, Kurz W. Acta Materiala 2001; 1051-1062.
- [3] Bezençon C, Wagnière J-D, Höbel M, Schnell A, Konter M, Kurz W. Single crystal coating of sx turbine blades by laser cladding technique, Materials for Advanced Power Engineering, 7th COST Conference 2002. p. 503-510.
- [4] Kurz W, Fisher DJ. Fundamentals of Solidification. Uetikon-Zuerich: Trans Tech Publications; 1998.
- [5] Rappaz M, David SA, Vitek JM, Boatner LA. Metallurgical Transactions 1989; 20 A:1125-1138.
- [6] Kurz W, Giovanola B, Trivedi R. Acta metall. 1986; 34:823-830.
- [7] Rappaz M, Boettinger WJ. Acta mater. 1999; 47:3205-3219.
- [8] Schnell A, Private communication.
- [9] Jansson B, Schalin M, Sundman B. J. Phase Equilibria 1993; 14:557.
- [10] Hunt JD. Materials Science and Engineering 1983; 65:75-83.
- [11] Gäumann M, Trivedi R, Kurz W. Materials Science and Engineering 1997; A226/228:763-769.
- [12] Bezençon C, Mokadem S, Drezet J-M, Sfera A, Kurz W. to be published.
- [13] Gandin C-A, Rappaz M. Acta Materiala 1994; 42:2233-2246.
- [14] Hauert A. Diploma Thesis. Institute of Materials: Swiss Federal Institut of Technology (EPFL); 2002.
- [15] Gandin C-A, Eshelman M, R. Trivedi. Metallurgical and Materials Transactions A 1996; 27:2727 - 2739.
- [16] Esaka H, Kurz W, Trivedi R, in *Solidification Processing*, J. Beech and H. Jones, Eds. London: The Institute of Metals, 1988, pp. 198-201.
- [17] Gandin C-A, Schaefer RJ, Rappaz M. Acta Materiala 1996; 44:3339-3347.
- [18] Bussac A, Gandain C-A. Materials Science and Engineering A 1997; 237:35-42.